Natural Rubber-Based Ionogels

TK. N. Tran[1,2], A. Guyomard-Lack[3], C. Cerclier[3], B. Humbert[3], G. Colomines[1], J-F. Pilard[2], R. Deterre[1], J. Le Bideau[3,*] and E. Leroy[4,*]

[1]*UBL, IUT of Nantes, CNRS, GEPEA, UMR 6144, 2 Avenue du professeur Jean ROUXEL, BP 539, 44475 Carquefou, France.*
[2]*UBL, University of Maine, UMR CNRS 6283, Institute of Molecules and Materials of Le Mans, Avenue Olivier Messiaen, 72085 Le Mans Cedex 9, France*
[3]*Institut des Matériaux Jean Rouxel (IMN), Université de Nantes, CNRS, 2 rue de la Houssinière, BP 32229, 44322 Nantes cedex 3, France*
[4]*UBL, CNRS, GEPEA, UMR 6144, CRTT, 37, Boulevard de l'Université, 44606 St Nazaire Cedex, France*

Received July 08, 2017; Accepted October 12, 2017

ABSTRACT: Natural rubber (NR), besides being an abundant renewable resource for the elastomer industry, can be a potential resource for the design of innovative biobased polymer networks. The present work is based on "telechelic" liquid natural rubber oligomers obtained by controlled chemical degradation of NR. The chain ends of such oligomers can then be functionalized (with acrylate functions in the present case) and reacted with multifunctional crosslinkers in order to form networks. What's more, the initial solubility of such thermosetting system in an ionic liquid (IL) can be used for the formulation of ionogels. Such solid networks typically containing 80% of IL were produced, resulting in high ionic conductivity performances. The oligomer chain length was shown to affect IL fragility due to confinement and specific interactions of ions with the host polymer network.

KEYWORDS: Natural rubber, oligomers, ionogels, confinement, ionic conductivity

1 INTRODUCTION

Natural rubber (NR) is an abundant renewable resource for the elastomer industry, and can be a potential carbon-neutral resource if one succeeds in recycling vulcanized rubber in an economically viable manner. Besides the traditional usage of NR in tire manufacturing, there has been other research dedicated to the direct use of natural rubber as a raw biomass resource for the design of novel biobased polymeric materials [1–6]. Such materials are based on "telechelic" liquid natural rubber, defined as a low molecular weight NR of approximately 10^3–10^4 g/mol, and bearing terminal groups capable of being used in further chain extension and crosslinking [7]. These novel biobased polymers are mostly hydroxy-telechelic NR-based polyurethanes (PUs) with final aspects such as elastomers [5–6], foams [8], interpenetrating polymer network (IPN) [4] and block copolymers [2]. Besides, it is noteworthy that the same chemistries have been applied to vulcanized rubber of waste tire to obtain hydroxyl-telechelic oligomers [9] used for the formulation of PU foams [10].

More recently, acrylate-telechelic natural rubber (AcTNR) oligomers have been synthetized and reacted with multifunctional acrylate crosslinkers such as trimethylolpropane triacrylate (TMPTA) in order to obtain thermoset networks with a glass transition temperature close to –60 °C [11]. In the present work we investigate the use of the thermosetting system AcTNR/TMPTA in combination with an ionic liquid (IL) for the elaboration of ionogels. This emerging family of solid ionic liquid-based biphasic materials [12] has attracted much attention due to their remarkable solid-state ionic conductivity properties: the confinement of ILs inside porous polymer network was shown to provide solid membranes endowed with the conductive properties, sometimes enhanced, of the pristine ILs [13, 14].

2 EXPERIMENTAL

2.1 Materials

1-Ethyl-3-methylimidazolium acetate IL (EMIm Ac, 98%, Solvionic), trimethylolpropanetri acrylate (TMPTA, Aldrich), methyl ethyl ketone peroxide

*Corresponding authors: eric.leroy@univ-nantes.fr; jean.lebideau@cnrs-imn.fr
DOI: 10.7569/JRM.2017.634174

 DOI: 10.7569/JRM.2017.634174

(MEKP, Aldrich), Cobalt octoate (trade name: COB 6, SF Composites) were used without further purification. Acrylate-telechelic natural rubber (AcTNR) oligomers (Mn = 1300 g/mol, 1900 g/mol, 2400 g/mol) were synthesized by using procedures previously described in detail [11]. Briefly stated, oligomers of natural rubber were first obtained by controlled degradation with periodic acid (H_5IO_6) in THF. In a second step, hydroxy-telechelic natural rubber (HTNR) oligomers were obtained by hydrolysis. Finally, acrylate-telechelic natural rubber (AcTNR) oligomers were obtained by reaction of HTNR with acryloylchloride. The structure of the AcTNR oligomers is shown in Figure 1. The controlled acidic degradation conditions used allowed the production of three grades of (AcTNR) of different average degrees of polymerization (m = 16, m = 25 and m = 32, corresponding respectively to average molecular weight Mn = 1300 g/mol, 1900 g/mol and 2400 g/mol).

2.2 Synthesis of Ionogels

Two series of ionogels containing 80% wt of EMIm Ac were produced. This IL content was chosen in order to obtain a "salt-in-polymer" solid electrolyte, which is a key concept of ionogels. It allowed obtaining a high IL/polymer ratio, without leading to a "polymer-in-salt" structure. The first series was obtained varying the TMPTA/AcTNR mass ratio (from 40/60 to 80/20) using the AcTNR with m = 32, and a second series varying the size of the AcTNR oligomer at a fixed TMPTA/AcTNR molar ratio of 8.1 (leading to 3 different TMPTA/AcTNR mass ratios of 65/35 for m = 16, 56/44 for m = 25, and 50/50 for m = 32).

In all cases, the procedure was the following: the TMPTA/AcTNR thermosetting system and cobalt octoate (0.2% wt) were vigorously mixed in 1-ethyl-3-methylimidazolium acetate (EMIm Ac) by using a vortex at a speed of 2500 rpm for 5 minutes at room temperature. The resulting solutions containing 80% wt of EMIm Ac and 20% wt of thermosetting system were translucent at room temperature (and fully transparent above 50 °C), indicating the solubility of AcTNR and TMPTA in the IL. The MEKP solution was added to the reaction mixture containing 80% wt of EMIm Ac and vigorously stirred for 30 seconds. The mole ratio of (double bond)/(MEKP) was kept at 30. The resultant mixture was then poured into a silicon mold. The curing reaction was kept at 80 °C in a closed oven purged with nitrogen gas for 5 hours.

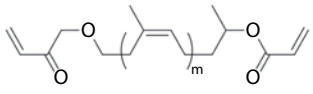

Figure 1 Structure of the acrylate-telechelic natural rubber (AcTNR) oligomers.

This processing strategy allows confining the IL in the host polyacrylate network in a single step. It is also expected to be more efficient than a two-step process in which the network is polymerized first, before subsequent IL impregnation. This would make it difficult to obtain such a high final content of IL confined in a porous network at the nanometer scale (see below).

The resulting solid ionogel samples were stored under dry atmosphere. The ionogels' composition is noted as follows: [host network]/IL wt%. Since the host networks arise from TMPTA/AcTNR mixture, the notation is [TMPTA/AcTNR wt% ratio]/IL wt%, the IL wt% being respective to the total mass of ionogel. Thus, here all ionogels correspond to [TMPTA/AcTNR]/80.

2.3 Mechanical Properties

A dynamic mechanical analyzer (DMA, Q500, TA Instruments) was used for all mechanical tests:

- Uniaxial tensile tests were conducted on rectangular samples (length ≈ 15 mm, width ≈ 7 mm, thickness ≈ 1 mm) using film tension clamps supported by cyanoacrylate adhesive to facilitate gripping during testing. All tensile tests were conducted in controlled force mode with a preload of 0.01 N and a force ramp rate of 0.05 N/min. All the tests were replicated three times.
- Compression tests were performed on cylindrical samples (diameter 11 ≈ mm, thickness ≈ 2 mm) compressed using a parallel plate measuring system at room temperature. All tests were conducted in controlled force mode with a preload of 0.01 N and a force ramp rate of 1 N/min until reaching the limit force (18 N) of DMA.
- Finally, dynamic compression analysis was carried out on the same cylindrical samples to determine the storage moduli of ionogels in the linear viscoelastic region. Specimens were tested using a parallel plate measuring system at room temperature. All dynamic tests were conducted in an amplitude sweep (from 2 µm to 100 µm) with a preload of 0.01 N and a frequency of 1 Hz.

2.4 Ionic Conductivity

The ionic conductivities were determined by complex impedance spectroscopy (CIS) using a BioLogic VMP2 multichannel potentiostat by varying the temperature from –20 °C to 90 °C. The frequency range used for

impedance measurements was 184 kHz –20 mHz and the amplitude used was 7 mV. Before any measurement, they were dried for 18 hours under vacuum (4 mbar) at 50 °C.

2.5 FTIR

Fourier transform infrared spectroscopy (FTIR) was performed on a Bruker Vertex 70 spectrometer in the attenuated total reflection mode (ATR). The ATR accessory used was a diamond Harnick 7 reflections device (ConcentratIRTM). The spectra resulted from averages of 100 scans at 4 cm^{-1} resolution, between 600 and 6000 cm^{-1}. Herein we show only the 1000–1800 cm^{-1} range.

3 RESULTS AND DISCUSSION

The mechanical properties of the ionogels are illustrated in Figure 2, Figure 3 and Table 1. Figure 2a,b shows the tensile and compressive stress-strain curves obtained for the first series of ionogels (varying TMPTA/AcTNR mass ratio). The curves obtained for the second series of ionogels (of varying oligomer size) are not shown for the sake of clarity, but the same trend was observed. When the network density increases (due to higher TMPTA/AcTNR mass ratio, or lower oligomer size), a stiffening of the material is observed.

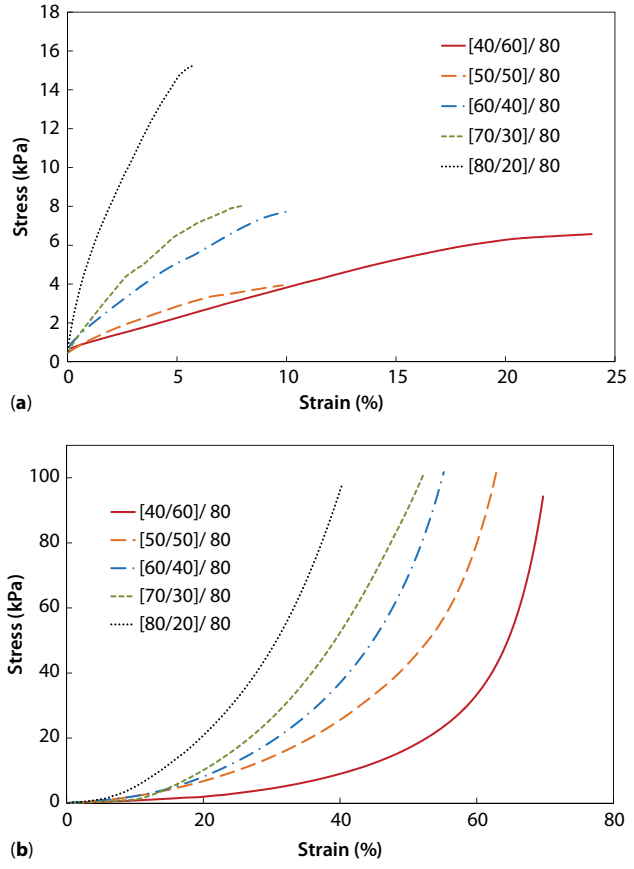

Figure 2 Tensile (**a**) and compression (**b**) test curves of ionogels containing 80% wt of EMIm Ac obtained for various TMPTA/AcTNR mass ratios using the AcTNR with m = 32.

The dynamic compression test curves at 1 Hz are also not shown here. Only the linear domain storage modulus values are reported in Table 1, along with the Young's modulus and elongation at break estimated from tensile tests. The elongation at break was typically around 10% for all samples except for the lowest TMPTA/AcTNR mass ratio. The Young's modulus and storage modulus values (ranging from 30 to 273 kPa for tensile tests, and from 45 to 157 kPa for dynamic compression tests) show a more important sensitivity to network structure.

Both can be used to evaluate the apparent mesh size [15] since the modulus E is related to the crosslink density ν (mole.m^{-3}):

$$E = \frac{3RTv}{2} \quad (1)$$

where R is the gas constant 8,32 J.mol^{-1}.K^{-1}.

Therefore, the apparent mesh size l can be roughly evaluated as follows:

$$l = \sqrt[3]{\frac{1}{v * N_a}} = \sqrt[3]{\frac{3RT}{2E * N_a}} \quad (2)$$

where N_a is the Avogradro constant ($6.02*10^{23}$).

The calculated values of l reported in Table 1 range from 2.8/3.4 to 5.9/5.4 nm depending on the modulus used. Such values confirm that the ionic liquid is confined in the network at the nanometer scale. The differences between the values obtained from the Young's

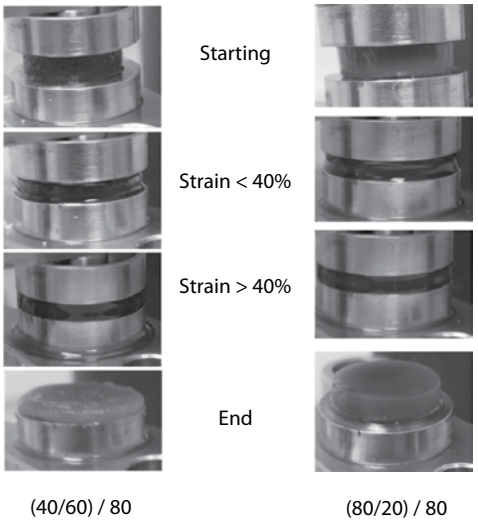

Figure 3 Behavior in compression tests. The ionic liquid is expelled from the network for compression strain above 40%.

 DOI: 10.7569/JRM.2017.634174

Table 1 Mechanical properties and estimated mesh sizes of the ionogels containing 80% wt of EMIm Ac.

Network's formulation		Tensile behavior		Compression behavior	Estimated mesh size	
Oligomer size m	TMPTA/ AcTNR (wt/wt)	Young's modulus (± 5 kPa)	Elongation at break (± 1%)	Storage modulus (1Hz) (± 5 kPa)	From tensile Young's modulus (nm)	From Compression Storage modulus (nm)
32	40/60	30	23	45	5.9	5.2
	50/50	45	11	50	5.2	5.0
	60/40	71	9	54	4.4	4.9
	70/30	117	10	93	3.8	4.0
	80/20	273	7	157	2.8	3.4
32	50/50	36	10	50	5.6	5.0
25	56/44	67	9	60	4.5	4.7
16	65/35	86	9	80	4.2	4.3

and storage moduli allow estimating the overall uncertainty. We should also point out that due to the radical curing reaction, a distribution of mesh sizes is probably present in each sample. Nevertheless, we rationalize the tendencies, not absolute values. For the m = 32 series, the mesh size decreases while increasing the amount of TMPTA crosslinker and reducing the amount of AcTNR. Consistently, for the TMPTA/AcTNR mole ratio of 8.1 series, the mesh size decreases when oligomer size decreases from 32 to 16.

During compression tests (Figure 2b), due to the very high deformability of the networks (up to 70% in some cases), it was observed that the ionic liquid can be expelled from the network at high strain. Figure 3 shows examples of test curves for two ionogels. It can be observed that the ionic liquid starts to flow out of the materials only when a 40% compressive strain is reached. At the end of the test, a porous sponge-like material is observed.

The ionic conductivity properties are illustrated in Figure 4 and Figure 5. All conductivities of ionogels fall in the same range, i.e., only 6 to 8 times lower than the bulk ionic liquid, while being solid. It is worth pointing out that reported conductivities refer to the whole ionogel, which is made of 20 wt% of host network and 80 wt% of IL.

The conductivity follows the typical non-Arrhenius behavior and is well described by the Vogel-Tammann-Fulcher (VTF) equation:

$$\sigma = \sigma_0 \exp\left[-\left(\frac{DT_0}{T - T_0}\right)\right] \quad (3)$$

where σ_0 is the theoretical conductivity at infinite temperature, T_0 is the ideal glass transition temperature and D is the fragility index.

The values obtained for these parameters are summarized in Table 2. D is inversely proportional to the fragility of the liquid [16] and is related to the temperature dependence of the dynamics of the liquid that affect ion transport.

Considering first the second series of ionogels, it appears that conductivities are higher for smaller initial oligomer size (m values), consistently with increased fragility (lower D values) and a decreased average mesh size (5.3 to 4.2 nm).

Now, for the first series of ionogels synthesized with m = 32, with a range of compositions leading to mesh sizes between 5.5 and 3.1 nm, although the mesh size decreased when a relative amount of crosslinker TMPTA increases, all conductivities and fragilities fall in the same range. Within this first series, fragility decreases (D value increases) when mesh size decreases. The highest D value and lowest conductivity is obtained for ionogel [80/20]/80. It thus seems to appear, from a comparison of tendencies of the first and second series, that a too important TMPTA crosslinker content slightly quenches the conductivity. It is difficult to reach more precise conclusions since the conductivities are quite close to each other, and also since the crosslinker shows a chemical feature different from the spacer, thus modifying the chemical features of the host network. We also have to point out that Table 2 reports two sets of VTF parameters obtained for two sets of synthesis for ionogel [50/50]/80, showing the overall uncertainty.

The results of FTIR spectroscopy allow investigating the interaction of EMIm Ac with the confining network (Figure 6). We consider here some specific bands for the second series of ionogels (Figure 6b,c and d). Note that similar trends were observed for the first series of ionogels:

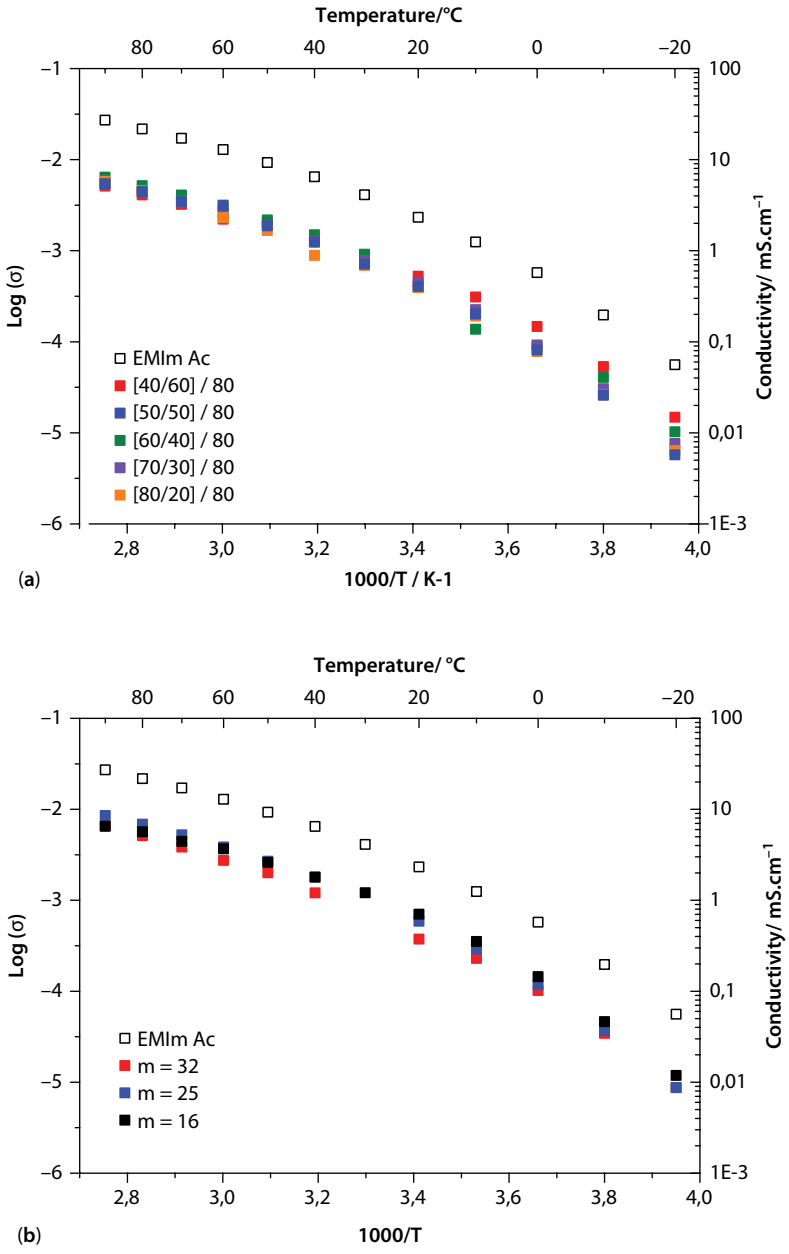

Figure 4 Ionic conductivities for first (**a**) and second (**b**) series of ionogels, compared to the bulk ionic liquid.

- The spectrum of unconfined EMImAc (black line, Figure 6b) shows two bands at 1560 cm^{-1} and 1574 cm^{-1} which correspond to the OCO^- asymmetric stretching of acetate anions non-interacting and interacting, respectively,with the imidazolium cation [17]. These anions' bands are only slightly modified upon confinement. Although, for the largest spacer (m = 32), the band's shape is almost the same as for the unconfined IL.
- For the cation of the unconfined IL, two bands are displayed at 1375 and 1324 cm^{-1} (black line, Figure 6c), assigned to modes involving (H-C7-H methyl) groups of imidazolium [17, 18]. In the ionogels' spectra (green, blue and red lines in Figure 6c), the vibrational frequencies of these two bands are again only slightly modified (the band at 1375 cm^{-1} shifts to 1379, 1380 and 1377 cm^{-1}, for m = 16, 25, 32 respectively), with again the lowest shift for the largest mesh size.
- The band at 1177 cm^{-1} for unconfined IL is also ascribed to the cation (Figure 6d). It involves $N_1C_2H_{11}$ with shifts to 1173 cm^{-1} for m = 16 and 25, and to 1175 cm^{-1} for m = 32.

Overall, it appears that the shifts appear more clearly for the smallest mesh sizes, while for the largest

 DOI: 10.7569/JRM.2017.634174

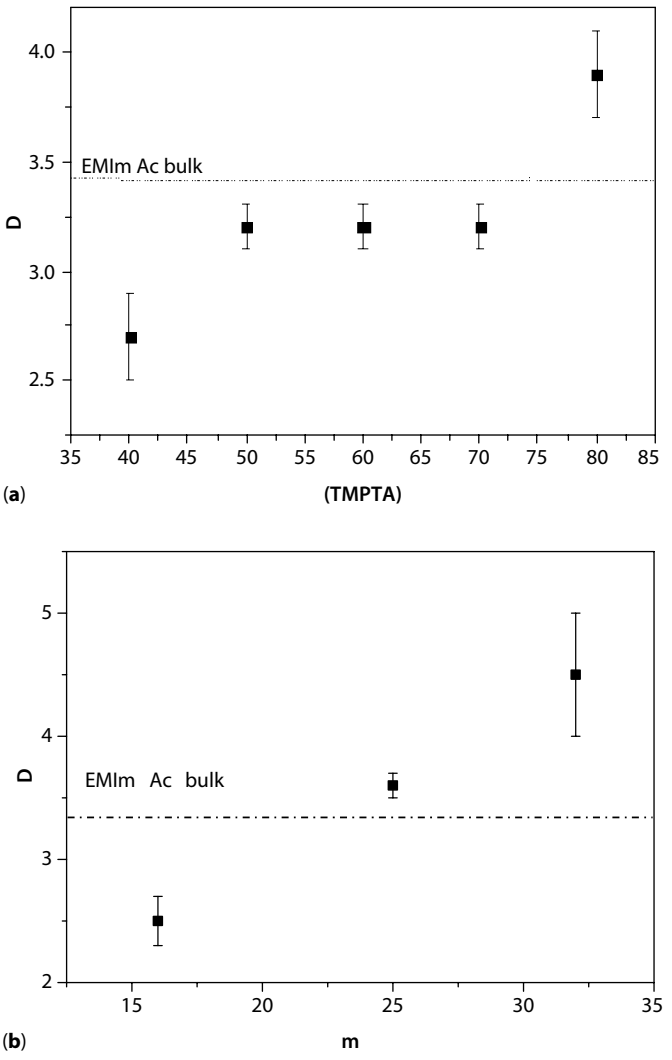

Figure 5 Estimated values of parameter D as a function of TMPTA ratio (**a**, first series of ionogels) and oligomer size (**b**, second series of ionogels).

we observe an average stemming from IL at host network neighborhood and bulk-like IL. Although these modifications are slight, the shift from 1177 to 1173 cm^{-1} for the cation in ionogel m = 16 could be related to the largest decrease of D index for the same ionogel.

4 CONCLUSIONS

Ionogels were synthesized by nanoscale confinement of the ionic liquid 1-ethyl-3-methylimidazolium acetate (EMImAc) in a natural rubber-based polyacrylate matrix. The structure of this partially biobased confining network consisting of acrylate-telechelic natural rubber (AcTNR) oligomers crosslinked with trimethylolpropane triacrylate (TMPTA) can be tuned by adjusting the AcTNR/TMPTA ratio, or the AcTNR oligomer size. This results in an average mesh sizes in the 3–6 nm range according to the mechanical properties of the ionogels, which could be compressed up to 40% without breakage or leakage of the ionic liquid.

The ionic conductivity of the ionogels (containing 80% of confined ionic liquid) is only 6 to 8 times lower than that of bulk ionic liquid, while being a solid material. Modeling the temperature dependence of the conductivity by the VTF equations shows that tuning the structure of the network leads to significant modifications of the ionic liquid's fragility, affecting transport properties. Analysis by FTIR spectroscopy shows specific shifts from the bands of anions and cations. The largest shifts are observed for the smallest mesh sizes, while for the largest mesh size an average from IL at host network neighborhood and bulk-like IL appears. This first study on high loadings of ionic liquid confined in natural rubber-based network opens up perspectives for new high added value applications of this natural polymer.

Table 2 Estimated values of the VFT model parameters.

		Ln σ_0	D	T_0/K	Average mesh size (nm)
	EMImAc	–6.8	3.4 +/–0.1	188 +/–1	–
m = 32	[40/60]/80	–9.1	2.7 +/–0.2	193 +/–3	5.5
	[50/50]/80	–8.3	3.2 +/–0.1	194 +/–1	5.1
	[60/40]/80	–8.3	3.3 +/–0.1	191 +/–1	4.6
	[70/30]/80	–8.5	3.2 +/–0.1	192 +/–1	3.9
	[80/20]/80	–7.9	3.9 +/–0.2	186 +/–1	3.1
m = 32	[50/50]/80	–7.5	4.5 +/–0.5	179 +/–4	5.3
m = 25	[56/44]/80	–7.7	3.6 +/–0.1	190 +/–1	4.6
m = 16	[65/35]/80	–8.7	2.5 +/–0.2	200 +/–2	4.2

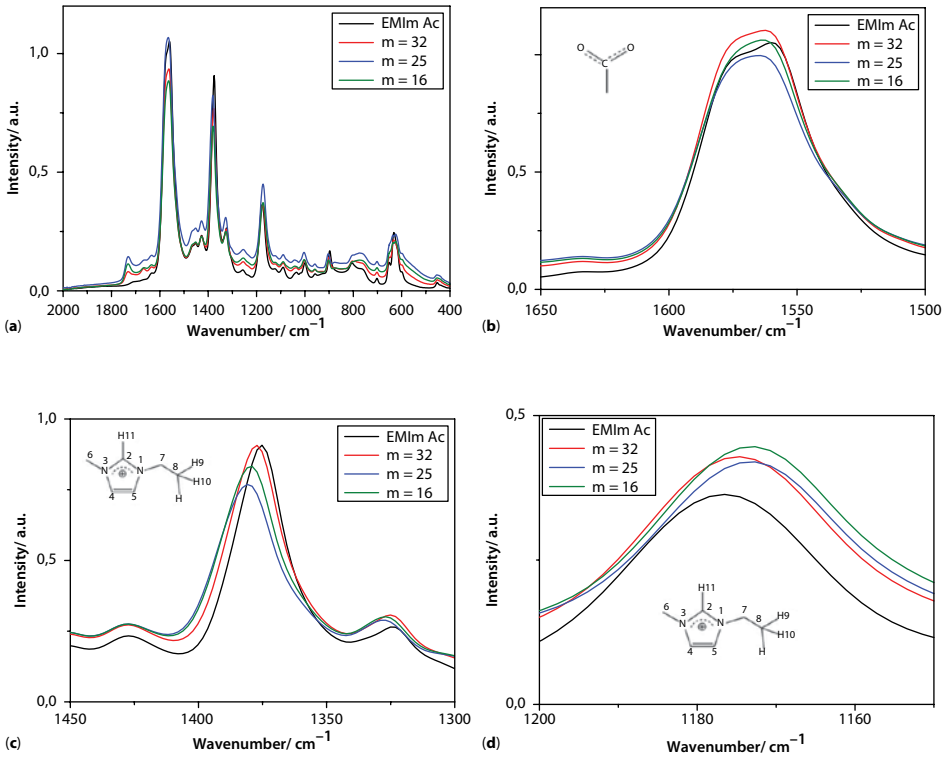

Figure 6 FTIR spectra of the second series of ionogels (a) and specific bands of the ionic liquid (b,c,d).

AKNOWLEDGMENTS

We are grateful for the financial support from the MATIERES project funded by the "Région Pays de la Loire" council. We also thank the Ionic Liquids and Polymers (GDR LIPs) French Research Consortium.

REFERENCES

1. R. Jellali, I. Campistron, P. Pasetto, A. Laguerre, F. Gohier, C. Hellio, J.F. Pilard, and J.L. Mouget, Antifouling activity of novel polyisoprene-based coatings made from photocurable natural rubber derived oligomers. *Prog. Org. Coat.* **76**, 1203–1214 (2013).
2. W. Chumeka, P. Pasetto, J.F. Pilard, and V. Tanrattanakul, Bio-based triblock copolymers from natural rubber and poly(lactic acid): Synthesis and application in polymer blending. *Polymer* **55**, 4478–4487 (2014).
3. W. Panwiriyarat, V. Tanrattanakul, J.F. Pilard, P. Pasetto, and C. Khaokong, Effect of the diisocyanate structure and the molecular weight of diols on bio-based polyurethanes. *J. Appl. Polym. Sci.* **130**, 453–462 (2013).
4. V.B. Pillai and D.J. Francis, Interpenetrating polymer networks based on liquid natural rubber. 1. Synthesis

and effect of NCO/OH ratio on physical and mechanical properties. *Angew. Makromol. Chem.* **219**, 67–76 (1994).
5. P. Rajalingam, G. Radhakrishnan, and J.D. Francis, Thermoset polyurethanes from hydroxyl-terminated natural rubber. *J. Appl. Polym. Sci.* **43**, 1385–1386 (1991).
6. T. Ravindran, M.R.G. Nayar, and D.J. Francis, Segmented block copolymers based on natural-rubber. *J. Appl. Polym. Sci.* **42**, 325–333 (1991).
7. H.M. Nor and J.R. Ebdon, Telechelic liquid natural rubber: A review. *Prog. Polym. Sci.* **23**, 143–177 (1998).
8. A. Saetung, A. Rungvichaniwat, I. Campistron, P. Klinpituksa, A. Laguerre, P. Phinyocheep, and J.F. Pilard, Controlled degradation of natural rubber and modification of the obtained telechelic oligoisoprenes: Preliminary Study of Their Potentiality as Polyurethane Foam Precursors. *J. Appl. Polym. Sci.* **117**, 1279–1289 (2010).
9. F. Sadaka, I. Campistron, A. Laguerre, and J.F. Pilard, Controlled chemical degradation of natural rubber using periodic acid: Application for recycling waste tyre rubber. *Polym. Degrad. Stabil.* **97**, 816–828 (2012).
10. T.K.N. Tran, J.F. Pilard, and P. Pasetto, Recycling waste tires: Generation of functional oligomers and description of their use in the synthesis of polyurethane foams. *J. Appl. Polym. Sci.* **132**, 11 (2015).
11. T.K.N. Tran, G. Colomines, E. Leroy, A. Nourry, J.F. Pilard, and R. Deterre, Rubber-based acrylate resins: An alternative for tire recycling and carbon neutral thermoset materials design. *J. Appl. Polym. Sci.* **133**, 7 (2016).
12. J. Le Bideau, L. Viau, and A. Vioux, Ionogels, ionic liquid based hybrid materials. *Chem. Soc. Rev.* **40**, 907–925 (2011).
13. A. Guyomard-Lack, B. Said, N. Dupre, A. Galarneau, and J. Le Bideau, Enhancement of lithium transport by controlling the mesoporosity of silica monoliths filled by ionic liquids. *New J. Chem.* **40**, 4269–4276 (2016).
14. A. Guyomard-Lack, N. Buchtova, B. Humbert, and J. Le Bideau, Ion segregation in an ionic liquid confined within chitosan based chemical ionogels. *Phys. Chem. Chem. Phys.* **17**, 23947–23951 (2015).
15. J.Y. Li and D.J. Mooney, Designing hydrogels for controlled drug delivery. *Nat. Rev. Mater.* **1**, 17 (2016).
16. C.A. Angell, Formation of glassed from liquids and biopolymers. *Science* **267**, 1924–1935 (1995).
17. L.J. Bellamy, *The Infrared Spectra of Complex Molecules, Volume Two Advances in Infrared Group Frequencies*, Springer, Netherlands (1980).
18. N.R. Dhumal, H.J. Kim, and J. Kiefer, Molecular interactions in 1-ethyl-3-methylimidazolium acetate ion pair: A density functional study. *J. Phys. Chem. A* **113**, 10397–10404 (2009).